Available online at www.sciencedirect.com
ScienceDirect
Cement and Concrete Research 36 (2006) 1653–1660
Cement and Concrete Research

Non-destructive monitoring of fiber orientation using AC-IS: An industrial-scale application

Nilufer Ozyurt [a,b,*], Thomas O. Mason [c], Surendra P. Shah [b]

[a] Faculty of Civil Engineering, Istanbul Technical University, Ayazaga Kampusu, Istanbul, 34469, Turkey
[b] Center for Advanced Cement Based Materials, Northwestern University, Evanston, IL, 60208, USA
[c] Department of Materials Science and Engineering, Northwestern University, Evanston, IL, 60208, USA

Received 9 July 2005; accepted 29 May 2006

Abstract

A comprehensive study has been undertaken to investigate the ability of AC-impedance spectroscopy (AC-IS) to non-destructively monitor the fiber dispersion of conductive fiber-reinforced cement-based materials. Previous work showed that AC-IS effectively monitors various fiber dispersion issues in lab-scale steel fiber-reinforced specimens. In this part of the study, AC-IS was used to study fiber orientation in an industrial-scale pre-cast concrete beam. A conventional method–image analysis (IA)–was used to verify the results of AC-IS measurements. The results of AC-IS and IA were found to match very well in experimental uncertainty. Splitting tensile tests and bending tests were conducted on the parts of the beam to study the effects of fiber orientation on the mechanical performance. The results of the mechanical tests also confirmed the results of AC-IS with splitting tensile strengths increasing as the alignment of fibers increased.

Keywords: Dispersion; Image analysis; Spectroscopy; Fiber reinforcement; Mechanical properties

1. Introduction

The use of fibers for reinforcing cement-based materials has been widely studied in the last four decades. The advantages and effectiveness of fiber use is known and well documented. Better understanding of fiber-reinforced composite (FRC) systems has led to the extension of fiber use from non-structural to semi-structural applications such as pavements, industrial floors, wall panels, bridge decks, tunnels, pre-cast roof elements, etc. [1,2]. However, the use of FRC is still limited in spite of the advantageous features of fiber reinforcement [3,4].

Undoubtedly, the use of fiber-reinforced cement composites for structural components will be more common in the future with increasing understanding of material behavior and development of new technologies such as engineered fibers [5]. Some structural applications of FRC have already been made possible using special high-performance fiber-reinforced composite materials such as DUCTAL® [6].

However, further research is required for a comprehensive understanding and a more widespread use of fiber-reinforced cement-based materials. Quality assurance and quality control systems are needed to be able to further commercialize these composites. Fresh and hardened state properties should be well monitored. Good fiber dispersion, as well as good concrete quality, should be assured. This study is focused on non-destructive fiber dispersion monitoring for quality control purposes. A non-destructive electrical method (AC-IS) was used to study fiber orientation on a portion of an industrial-scale FRC beam which was supplied by a pre-cast concrete company. Experiments were conducted at Northwestern University (NU).

Alternating current-impedance spectroscopy (AC-IS) is an electrical characterization method that can be used to study various aspects of cement-based materials such as hydration development, pore structure [7], cracking (damage evolution) [8] and chloride ion diffusivity [9]. Recently, the use of AC-IS was extended to fiber dispersion monitoring, which is possible due to the dual-arc behavior that occurs with the inclusion of

* Corresponding author. Faculty of Civil Engineering, Istanbul Technical Univ., Ayazaga Kampusu, Istanbul, 34469, Turkey.
E-mail address: ozyurtnil@itu.edu.tr (N. Ozyurt).

0008-8846/$ - see front matter © 2006 Elsevier Ltd. All rights reserved.
doi:10.1016/j.cemconres.2006.05.026

Table 1
Concrete mix proportions

Cement (kg)	Water (kg)	Gravel (kg)	Sand (kg)	Fly Ash (kg)	SP (kg)	Fibers (kg)	VMA (kg)
321	142	545	509	151	1.7	59	0.2

conductive fibers [10,11]. Previous work of the authors showed that AC-IS can be used to monitor various fiber dispersion issues, including clumping, orientation and segregation in lab-scale specimens [12–14]. In this study, similar experiments were conducted on an industry-scale specimen to study the ability and potential of AC-IS to detect fiber orientation in structural components. The results show promise, suggesting that AC-IS can be developed as a non-destructive quality control technique in the near future. It should be noted that AC-IS can only be used for fiber dispersion monitoring when the fibers are conductive and the experimental configuration may vary depending on the size/geometry of the fibers and specimen under consideration.

2. Experimental study

A pre-cast fiber-reinforced concrete beam was used to study preferred orientation of fibers using AC-IS. CON/SPAN® Bridge Systems supplied a FRC beam that had been manufactured at their plant. The beam was cast and tested under four point bending by the company prior to be sent to NU. (Only a part of the whole beam was used for convenience of transportation and experimental study.) CON/SPAN® Bridge Systems provided the information regarding the materials and their properties. The dimensions of the full beam were 25.4×15.2×400 cm (10″×6″×13′). The fiber-reinforced beam was cast with self-compacting concrete using 1% Dramix® RC 65/60 (L=60 mm, AR=65) steel fibers. Round coarse aggregate with a maximum diameter of 9.5 mm and class C fly ash were used. The concrete was batched at the ready mix plant and the superplasticizer (polycarboxylic-based) and fibers were added at the factory where the beams poured and mixed for about 5 min at the maximum mixing speed (22 rpm). The mix used is given in Table 1.

Fig. 1 shows the beam after being tested under four-point bending. The right side of the beam, with a length of 71 cm (2′4″) was used for the orientation tests. First, AC-IS tests were carried out on the beam. Then, the beam was cut and image analysis and splitting tensile tests were done.

2.1. AC-IS

AC-IS is a non-destructive evaluation method in which an excitation voltage is applied over a range of frequencies to a specimen and the current response is measured. The data are then converted to real and imaginary values of impedance and plotted on a Nyquist plot. Fig. 2 shows a typical Nyquist plot for plain cement paste and steel fiber-reinforced cement pastes. The frequency is stepped from low (Hz) to high (MHz) such that each frequency generates a single datum in the so-called Nyquist plots (−imaginary vs. +real impedance), with frequency markers ($\log_{10} f$) as shown. The dual-arc behavior can be explained with reference to Fig. 2. The rightmost arc in both curves is associated with the electrode response and does not depend on the material properties. The bulk arcs (left of the electrode arc) are related to the material. In the absence of fibers, plain cement paste shows a single arc with a single low-frequency cusp. On the other hand, with the inclusion of conductive fibers, the specimen shows two bulk arcs that are separated by a high-frequency cusp. This behavior is called dual-arc behavior and it occurs due to the frequency dependent behavior of conductive fibers. Conductive fibers are insulating under low frequencies (Hz) of AC due to either an oxide film (e.g., on steel fibers) or a polarization layer (i.e., double layer/charge transfer resistance) forming at the fiber–electrolyte interface, while they are conductive under high frequencies (MHz) owing to displacement currents short-circuiting the oxide/polarization layer [10,15,16]. Further explanation of dual-arc behavior is available in the literature [10,17].

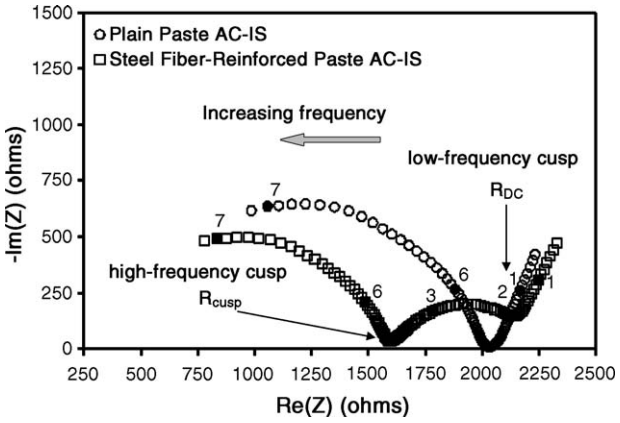

Fig. 2. Sample Nyquist curves for plain and steel fiber-reinforced cement pastes (w/c=0.40, fiber volume=0.35 vol.%).

In Fig. 2, the rightmost cusp (R_{DC}) in both plots is the matrix resistance (R_{DC}). The leftmost cusp (R_{cusp}) occurs only when conductive fibers are present and is the resistance of the composite (R_{cusp}). R_{DC} and R_{cusp} can be used to calculate the matrix conductivity (σ_m) and the composite conductivity (σ), respectively, as given below:

$$\sigma_m = \frac{1}{R_{DC}} \qquad \sigma = \frac{1}{R_{cusp}} \tag{1}$$

An intrinsic conductivity approach can be used to obtain the dispersion characteristics from the experimental data.

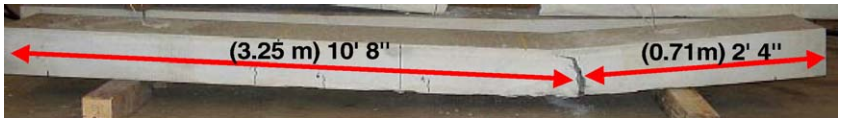

Fig. 1. Precast steel fiber-reinforced concrete beam after four-point bending test.

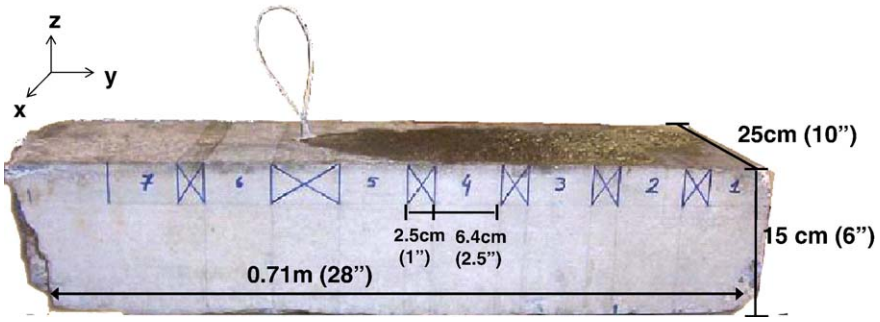

Fig. 3. Studied part of the pre-cast beam (AC-IS measurement locations are marked).

According to this approach, each particle geometry has a specific intrinsic conductivity which can be calculated based upon the geometrical parameters of the inclusion.

Douglas and Garboczi give the following relationship between the matrix normalized conductivity (σ/σ_m) and the intrinsic conductivity ($[\sigma]_\Delta$) for composites in the dilute limit [18]:

$$\sigma/\sigma_m = R_{DC}/R_{cusp} = 1 + [\sigma]_\Delta \phi, \qquad \Delta = \frac{\sigma_f}{\sigma_m} \tag{2}$$

In Eq. (2), σ is the composite conductivity, σ_m is the matrix conductivity, R_{DC} is the measured resistance of the matrix, R_{cusp} is the measured resistance of the composite, ϕ is the volume fraction of the fibers and $[\sigma]_\Delta$ is the "intrinsic conductivity" of the fibers. Δ is the ratio of the fiber conductivity to the matrix conductivity. In the case of perfectly conductive fibers, Δ approaches ∞, while it is approximately $-5/3$ for insulating fibers (right cylinders or prolate ellipsoids) for all aspect ratios greater than 10. For highly conductive fibers, $[\sigma]_\infty$ can be calculated knowing only the aspect ratio (AR = l/d, length over diameter) of the fiber using the modified Fixman equation [19]:

$$[\sigma]_\infty = \frac{1}{3}\left[\frac{2(AR)^2}{(3\ln\{4(AR)\}-7)} + 4\right] \tag{3}$$

It should be noted that Eq. (3) assumes the fibers are randomly oriented cylindrical fibers. Further information about the intrinsic conductivity approach and its utilization to obtain fiber dispersion characteristics can be found in the previous work of the authors [12–14]. In this study, matrix-normalized conductivity (σ/σ_m) profiles of the beam were obtained and compared for two directions to be able to define the state of fiber orientation in the beam.

Seven parts of the beam, each with a width of 6.4 cm (2.5″), were selected for electrical measurement as shown in Fig. 3. AC-IS measurements were obtained from all parts in two directions to obtain matrix-normalized conductivity profile of the beam. Fig. 3 shows the dimensions of the beam together with the studied sections.

2.1.1. AC-IS experimental setup

Fig. 4 shows the experimental setup for the AC-IS measurements. Stainless steel circular electrodes with radii of ~ 59 mm (2.3″) were used on top of the specimen. These electrodes were submerged in highly conductive NaCl aqueous solutions, but were not in direct contact with the beam surface. Several electrode configurations were examined and this configuration was found to be the most effective for this particular specimen and fiber geometry. Artificial reservoirs were created using sealing putty and filled with 1 M NaCl solution to provide good contact of electrodes and the specimen. A Solartron 1260 impedance/gain-phase analyzer was used, and the frequency was stepped from 100 mHz to 11 MHz under a voltage excitation of 1 V.

AC-IS measurements were obtained from both the X and Z directions for all seven regions. Fig. 5 shows the electrode positions and approximate current paths for the X and Z directions. Measurements were repeated two times to confirm the reproducibility of the results.

Fig. 6 shows the normalized conductivity profiles for the X and Z directions. The X axis shows the measurement points on the beam. Conductivity was found to be higher in the X direction than in the Z direction, suggesting preferred orientation of the fibers in the X direction. This behavior can be explained as follows. Previous work has shown that AC-IS is directionally sensitive meaning that the contribution of a fiber to conductivity is depend on its alignment relative to the direction of current. Higher conductivity in the X direction means that

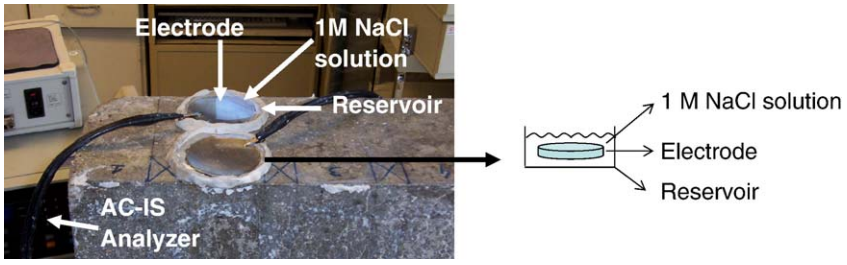

Fig. 4. AC-IS experimental setup.

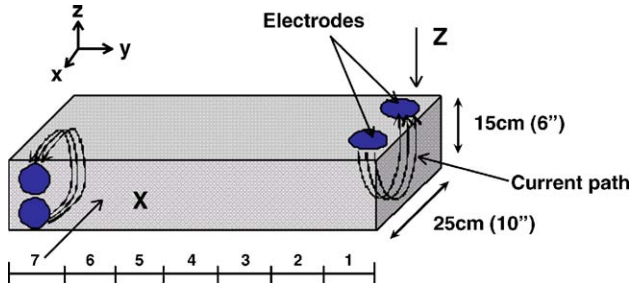

Fig. 5. Schematic of measurement directions and approximate current paths for *X* and *Z* directions.

fibers are more likely to align in this direction. This observation is expected, since previous studies have shown that fibers tend to align in the plane that is vertical to the casting direction [20]. It should be noted that the *Z* direction is the casting direction for this study. Another possible reason for variations in the matrix-normalized conductivity values can be variations in fiber contents at different parts of the beam. To check for this effect approximate fiber contents in different parts of the beam were determined and were found to be similar independent of location along the beam. Details are given in the next section.

To further study these findings, image analysis and mechanical tests were conducted on the specimen and the results are given in the next sections.

2.2. Image analysis

A straightforward technique was used for image analysis. First, the beam was cut into seven pieces, with the approximate dimensions of 8.9×15.2×25.4 cm (3.5″×6″×10″), as seen in the left hand side of Fig. 7 (the segments are numbered from 1 to 7). Then, each piece was cut into two parts vertically (part a and part b) with the dimensions of 8.9×12.7×12.7 cm (3.5″×5″×5″) to be used for image analysis and mechanical testing. 2.54 cm (1″) from the top of each specimen was removed using a saw to smooth the specimen surface for splitting tensile tests. The number of fibers on *XY* and *ZY* planes was counted for each piece. A schematic of studied planes is shown shaded in the right hand side of Fig. 7.

Fig. 8 shows *XY* and *ZY* planes of beam part 2. As seen in Fig. 8, the number of fibers on the *XY* plane is noticeably smaller than on the *ZY* plane, indicating a preferred alignment of fibers in the *XY* plane, as suggested by AC-IS measurements. Another reason for having fewer fibers on the *XY* plane could be segregation of fibers since the studied plane was close to the top surface. To check for this effect, specimen cross-sections were visually examined and no sign of fiber segregation was observed.

The number of fibers on a cross-section depends on the orientation of fibers in the plane. A relationship between the number of fibers and the orientation number is given as follows [21]:

$$\eta_\varphi = \frac{N_f * A_f}{V_f} \quad (4)$$

where: η_φ=orientation number, N_f=number of fibers per unit area (1/mm^2), A_f=cross-sectional area of a single fiber (mm^2) and V_f=fiber volume fraction (vol.%).

The numbers of fibers on the *XY* and *ZY* planes were counted to be able to calculate orientation numbers for each beam part using Eq. (4). Fig. 9 presents the results from these calculations for each part of the beam. Higher orientation number means more fibers oriented perpendicular to the plane under consideration. For instance, in Fig. 9, higher orientation numbers on the *ZY* planes means preferred orientation of fibers in the *X* direction.

As was expected, the orientation numbers were found to be lower in the *Z* direction, in agreement with AC-IS findings.

When Figs. 6 and 9 are compared, similar tendencies are observed. Both AC-IS and image analysis show preferred orientation in the *XY* plane. Orientation number profiles show very similar peaks and valleys with the matrix-normalized conductivity profiles for the *Z* direction, confirming AC-IS results.

In both Sections 2.1.1 and 2.2, the variations in matrix-normalized conductivity and orientation number values were attributed to the preferred orientation of fibers. Another reason for variations in these values may be differences in fiber content throughout the beam. To check for this effect, fiber contents in different parts of the beam were calculated. The number of fibers at each *XZ* face was counted (left hand side of Fig. 7, *XZ* sections), after the beam was cut into seven parts. Fiber content was found to be similar in each part of the beam. The number of fibers per unit area varied 7% from the average. On the other hand, normalized conductivity and orientation number values varied around ±20%, suggesting preferred orientation of fibers in the beam.

Fig. 10 shows the orientation number versus matrix-normalized conductivity relation, indicating a linear relationship, with an R^2 value of approximately 0.83.

2.3. Mechanical tests

Splitting tensile tests and three-point bending tests were conducted on the beam parts to study the effects of fiber

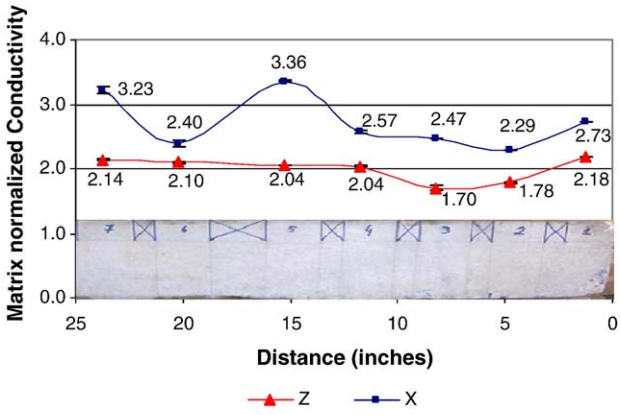

Fig. 6. Matrix-normalized conductivity profile of the beam for *X* and *Z* directions. R_{DC} varied 10% and 12% from the average for the *Z* and *X* directions, respectively.

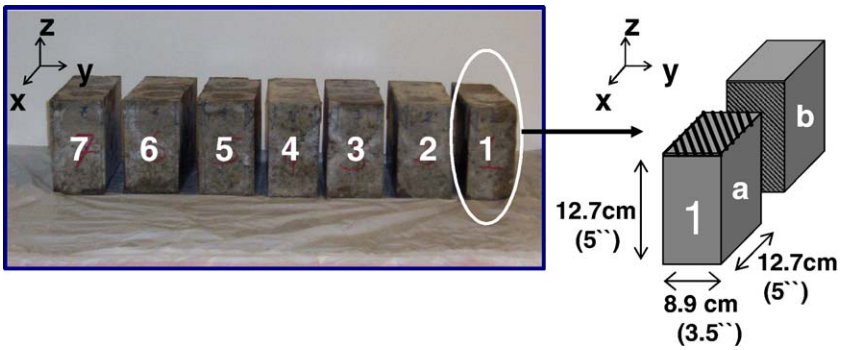

Fig. 7. Studied specimens with section numbering.

orientation on mechanical properties (Fig. 12). The beam was cut into parts for splitting tensile tests as was defined in Section 2.2 (see Fig. 7). Part (a) was loaded in the *X* direction, while part (b) loaded in the *Z* direction (casting direction) for each sample as shown in the right hand side of Fig. 12.

Splitting tensile tests were conducted according to a modified version of EN-12390-6. A closed-loop MTS testing machine was used with a 500 kN (110 kip) capacity load cell. Loading was applied under average lateral displacement control, which was monitored using two LVDTs (Linear variable displacement transducer) that had a maximum range of 2.5 mm. The LVDTs were fixed onto each side of the specimen and the lateral displacement in the *Y* direction was monitored as seen in Fig. 12.

Initially, loading was applied at a rate of 0.00025 mm/s. After the maximum stress was reached, the rate was increased to 0.001 mm/s (for the sake of time). Testing continued until a 2 mm lateral displacement was reached. Load and LVDT displacements were recorded for data analysis (Fig. 11).

Splitting tensile strength values were calculated using Eq. (5), and the splitting tensile strength profile of the beam was obtained (Fig. 12).

$$f_{ct} = \frac{2P}{\pi LD} \tag{5}$$

In Eq. (5), f_{ct} is stress (MPa), P is the maximum load (N), L is the length of the line of contact of the specimen (12.7 mm for this study) and D is the cross-sectional dimension (12.7 mm for this study) of the specimen.

When the specimen was loaded in the *X* direction the fibers aligned on the *XY* plane are effective in arresting cracks. When loaded in the *Z* direction, fibers on the *ZY* plane are the effective fibers. The number of fibers oriented in *XY* had been found to be higher than the number of fibers oriented in *YZ* plane. This may be the reason for the slight difference between the splitting tensile strength profiles in Fig. 12.

The results of the splitting tensile strength test were good representation of the orientation characteristics of the *XY* and *ZY* planes. However, additional tests (three-point bending)

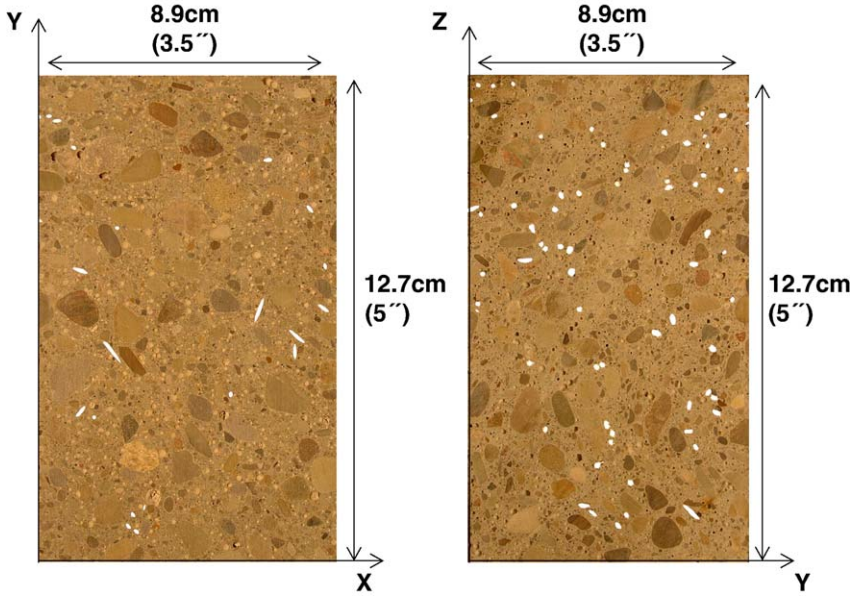

Fig. 8. The pictures of *XY* and *ZY* planes for the beam part 2.

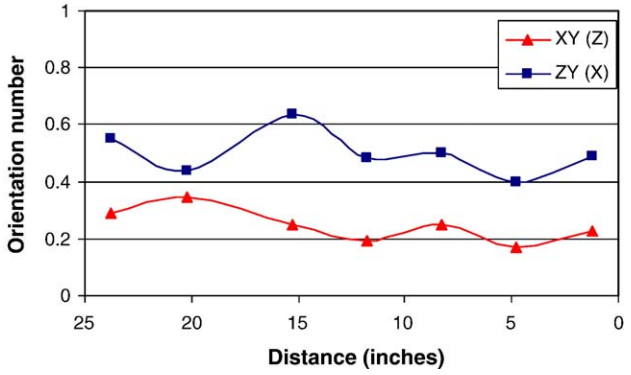

Fig. 9. Orientation number profiles of the fiber-reinforced concrete beam for the *X* and *Z* directions. Beam was cut into seven parts and the numbers of fibers on the *XY* and *ZY* faces were counted. Orientation numbers are calculated using Eq. (4) to mathematically express the orientation level in the *X* and *Z* directions using an alternate method (IA).

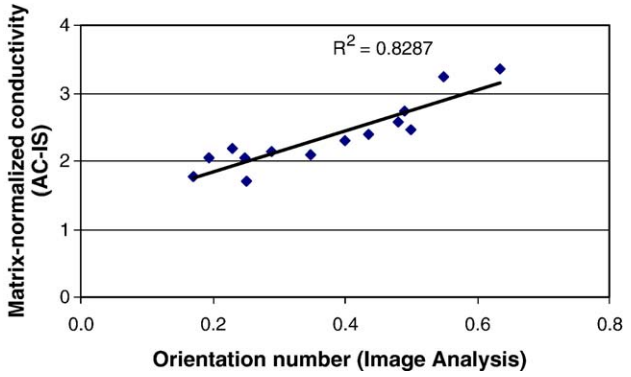

Fig. 10. Matrix-normalized conductivity versus orientation number (data from both the *X* and *Z* directions are plotted together).

were carried out on the specimens. The purpose of making additional tests was to more clearly observe the orientation characteristics in the single directions (*X*, *Z*) rather than planes (*XY*, *YZ*). Specimens with the dimensions of 2.5 × 2.5 × 12.7 cm

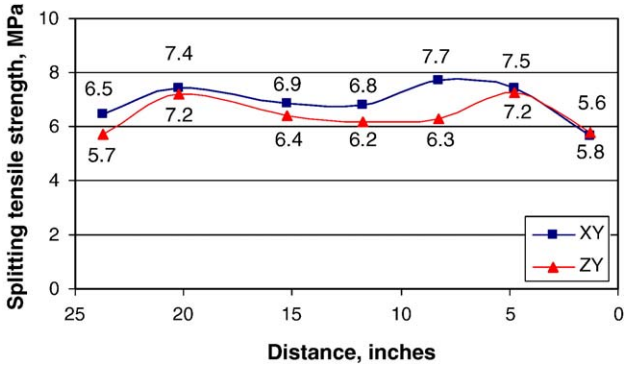

Fig. 12. Splitting tensile strength profiles of the fiber-reinforced precast beam. Load applied in two directions (*X*, *Z*) to obtain splitting tensile strength profiles of the beam.

(1″ × 1″ × 5″) were cut out of the beam parts 2, 5 and 6, and tested in the *X* and *Z* directions (casting direction) as seen in Fig. 13. The reason for using small beams was the limited number of specimens. A notch with a depth of 10 mm (40% of entire depth) was cut and an extensometer was used to measure CMOD. A closed-loop MTS testing machine was used. Loading was applied under CMOD control. Three replications were made for both the *X* and *Z* directions.

Fig. 14 shows the load versus CMOD curves for beam part 6. As seen in the figure when the load applied in the *X* direction, the specimen behaves in a very brittle manner due to the lack of the fibers in the *Z* direction. On the other hand, when load is applied in the *Z* direction, the specimen fails in a ductile manner owing to the fibers aligned in the *X* direction. Similar trends were obtained for other parts of the beam. Fig. 14 is a good representation of the effect of the fiber orientation on the mechanical performance. Finally, to compare the orientation characteristics in three directions, splitting tensile strength profile in the *Z* direction was estimated (using flexural strength data and Eq. (7)) and plotted with Fig. 12.

Flexural strength values were calculated using Eq. (6). In Eq. (6), $\sigma_{flexural}$ is stress, *M* is moment, *c* is the one half the beam depth (7.62 mm), *I* is moment of inertia, *P* is the load, *L* is the

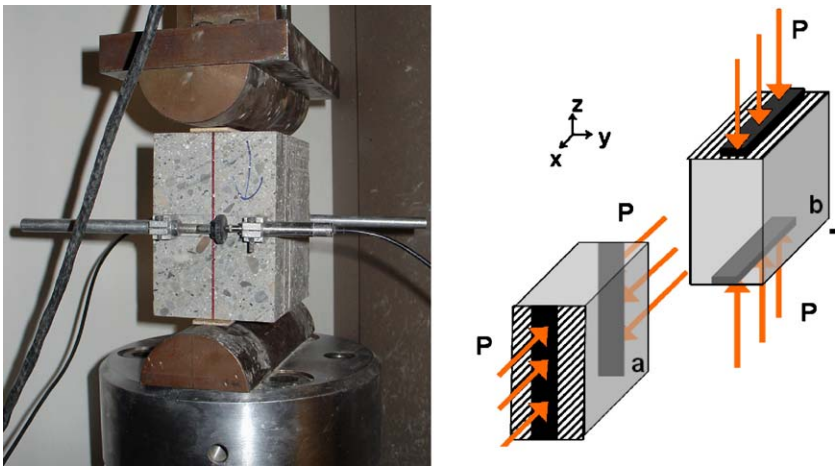

Fig. 11. Splitting tensile test set up with two LVDTs on each side.

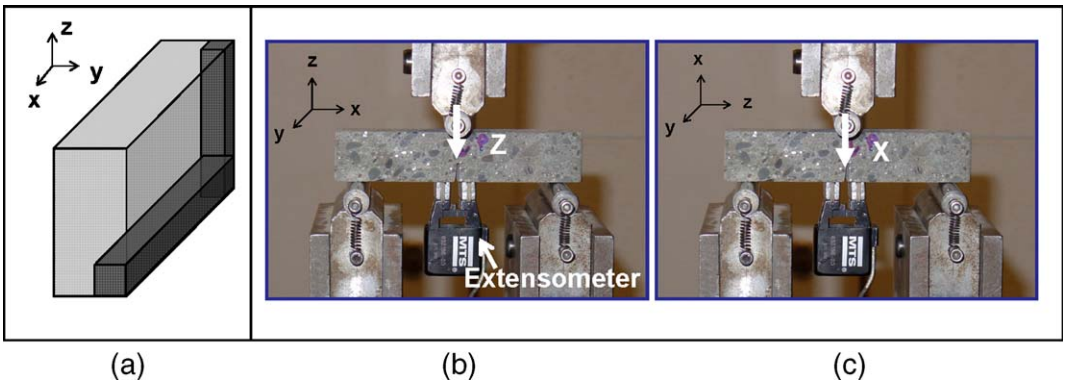

Fig. 13. Small beam specimens were cut out of the beam parts (a) and tested in the Z (b) and X directions (c).

length of the specimen span (101.6), w is the specimen width (25.4 mm) and d is the effective depth of the specimen (15.2 mm).

$$\sigma_{\text{flexural}} = \frac{Mc}{I} \qquad \left(M = \frac{PL}{4}, I = \frac{1}{12}wd^3\right) \tag{6}$$

The average ratio of splitting tensile strength values to the flexural strength values in the X direction (Eq. (7)) was calculated and found to be 0.67. This ratio and the observed flexural strength values were employed to estimate the splitting tensile values in the Z direction. This estimated profile is plotted together with Fig. 12 and is given in Fig. 15.

$$\left(\frac{\sigma_{\text{splitting}}}{\sigma_{\text{flexural}}}\right)_X = 0.67 \tag{7}$$

In Fig. 15, the legend shows the direction in which the specimen was tested and the direction of the fibers that are effective in arresting crack development. For instance, the closed circle data points were for samples tested in the X direction and the fibers aligned in the (XY) plane were effective in arresting the cracks. As seen in Fig. 15, the lowest values were obtained in the direction in which the fibers aligned in the Z direction were effective in arresting cracks. This behavior can be explained based on the image analysis results. The number of fibers aligned in the Z direction was small and therefore less effective in arresting cracks compare to the number of fibers aligned in the other directions.

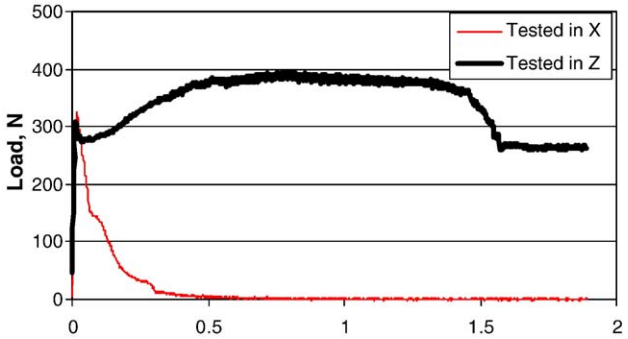

Fig. 14. Load versus CMOD relations from three-point bending test.

3. Conclusions

The use of AC-IS as a non-destructive technique to monitor fiber orientation was studied in an industrial-scale self-compacting steel fiber-reinforced concrete beam. The fiber orientation in the beam was described by means of matrix-normalized conductivity profiles in two directions. Results suggested a preferred orientation of fibers in the XY plane. This was expected based on previous results from other researchers. Image analysis was conducted to understand the extent to which AC-IS predicts fiber orientation. A linear relationship was found between the results verifying the ability of AC-IS to monitor fiber orientation. Splitting tensile tests and three-point bending tests were carried out on the beam to evaluate the effects of fiber orientation on the mechanical performance. Tensile strength was found to be lower in the poorly reinforced direction. Considering the results, the following statements can be made:

- AC-IS is an effective technique for monitoring fiber orientation in conductive fiber-reinforced cement-based materials.

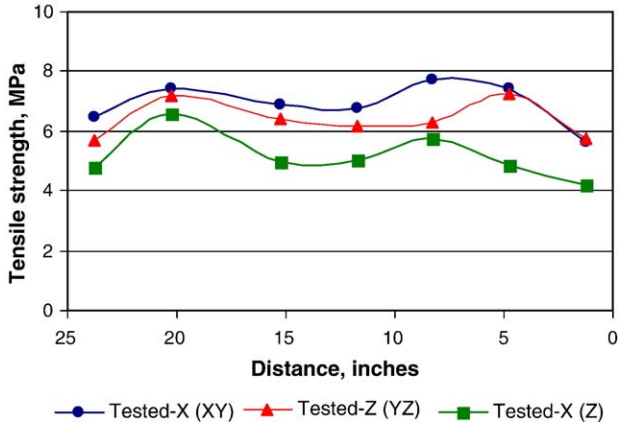

Fig. 15. Splitting tensile strength profiles of the precast beam. Splitting tensile strength in the direction that the fibers in the Z direction were effective in arresting cracks was estimated using the results of bending tests and Eq. (7).

- AC-IS and image analysis results match well, verifying the ability of AC-IS for fiber dispersion monitoring.
- The potential exists for AC-IS to be utilized as a non-destructive technique for quality control purposes.

Acknowledgements

The authors gratefully acknowledge CON/SPAN® Bridge Systems and Dave Brodowski for their support and contribution to this work. The first author also would like to acknowledge the financial support of TUBITAK (The Scientific and Technical Research Council of Turkey) and ITU (Istanbul Technical University). The authors are grateful to Dr. Leta Woo for helpful discussions.

References

[1] L. Ferrara, A. Meda, T. Lamperti, F. Pasini, in: R.F.M. di Prisco, G.A. Plizzari (Eds.), 6th RILEM Symposium on Fibre-Reinforced Concretes, BEFIB, RILEM Publications S.A.R.L, 2004, pp. 493–504.
[2] T. Teruzzi, E. Cadoni, G. Frigeri, S. Cangiano, G.A. Plizzari, in: R.F.M. di Prisco, G.A. Plizzari (Eds.), 6th RILEM Symposium on Fibre-Reinforced Concretes, BEFIB, RILEM Publications S.A.R.L, 2004, pp. 625–633.
[3] P. Gambarova, in: R.F.M. di Prisco, G.A. Plizzari (Eds.), 6th RILEM Symposium on Fibre-Reinforced Concretes, BEFIB, RILEM Publications S.A.R.L, 2004, pp. 125–140.
[4] L. Cominoli, F. Minelli, P. Riva, in: R.F.M. di Prisco, G.A. Plizzari (Eds.), 6th RILEM Symposium on Fibre-Reinforced Concretes, BEFIB, RILEM Publications S.A.R.L, 2004, pp. 787–798.
[5] A.E. Naaman, Engineered steel fibers with optimal properties for reinforcement of cement composites, J. Adv. Concr. Technol. 1 (3) (2003) 241–252.
[6] P. Casanova, J. Dugat, G. Orange, in: C.K.Y. Leung, Z. Li, J.-T. Ding (Eds.), International Symposium on High Performance Concrete, 2000, pp. 853–859.
[7] B.J. Christensen, R.T. Coverdale, R.A. Olson, S.J. Ford, E.J. Garboczi, H.M. Jennings, T.O. Mason, Impedance spectroscopy of hydrating cement-based materials: measurement, interpretation, and application, J. Am. Ceram. Soc. 77 (11) (1994) 2789–2804.
[8] A. Peled, J.M. Torrents, T.O. Mason, S.P. Shah, E.J. Garboczi, Electrical impedance spectra to monitor damage during tensile loading of cement composites, ACI Mater. J. 98 (2001) 313–322.
[9] J.M. Loche, A. Ammar, P. Dumargue, Influence of the migration of chloride ions on the electrochemical impedance spectroscopy of mortar phase, Cem. Concr. Res. 35 (9) 1797-1803.
[10] J.M. Torrents, T.O. Mason, A. Peled, S.P. Shah, E.J. Garboczi, Analysis of the impedance spectra of short conductive fiber-reinforced composites, J. Mater. Sci. 36 (2001) 4003–4012.
[11] J.M. Torrents, T.O. Mason, E.J. Garboczi, Impedance spectra of fiber-reinforced cement-based composites, Cem. Concr. Res. 30 (2000) 585–592.
[12] L.Y. Woo, S. Wansom, N. Ozyurt, B. Mu, S.P. Shah, T.O. Mason, Characterizing fiber dispersion in cement composites using AC-impedance spectroscopy, Cem. Concr. Compos. 27 (6) (2005) 627–636.
[13] N. Ozyurt, L.Y. Woo, B. Mu, S.P. Shah, T.O. Mason, Advances in concrete through science and engineering, in: K. Kovler, J. Marchand, S. Mindess, J. Weiss (Eds.), Proc. of the Int. Symp., Evanston, USA, vol.1, RILEM Publications, 24 March 2004, p. 263, on CD-ROM.
[14] N. Ozyurt, L.Y. Woo, T.O. Mason, S.P. Shah, Monitoring fiber dispersion in FRCs: comparison of AC-impedance spectroscopy and image analysis, ACI Materials Journal (in press).
[15] M.A. Campo, L.Y. Woo, T.O. Mason, E.J. Garboczi, Frequency-dependent electrical mixing law behavior in spherical particle composites, J. Electroceram. 9 (2002) 49–56.
[16] J.M. Torrents, T.O. Mason, E.J. Garboczi, Impedance spectra of fiber-reinforced cement-based composites. A modeling approach, Cem. Concr. Res. 30 (2000) 585–592.
[17] T.O. Mason, M.A. Campo, A.D. Hixson, L.Y. Woo, Impedance spectroscopy of fiber-reinforced cement composites, Cem. Concr. Compos. 24 (2002) 457–465.
[18] J.F. Douglas, E.J. Garboczi, Intrinsic viscosity and the polarizability of particles having a wide range of shapes, Adv. Chem. Phys. XCI (1995).
[19] A.D. Hixson, L.Y. Woo, M.A. Campo, T.O. Mason, E.J. Garboczi, Intrinsic conductivity of short conductive fibers in composites by impedance spectroscopy, J. Electroceram. 7 (2001) 189–195.
[20] S. Grunewald, J.C. Walraven, Case studies with self-compacting steel fiber reinforced concrete, Concrete Plant+Precast Technology (BFT), 2004, pp. 18–27.
[21] H. Krenchel, in: A. Neville (Ed.), RILEM, Symposium on Fibre Reinforced Cement and Concrete, The Construction Press Ltd, 1975, pp. 69–79.